Automatic Segmentation Using Non-Rigid Registration

Kilian M. Pohl[1], Sylvain Bouix[2], Martha .E. Shenton[2], W. Eric L. Grimson[1], and Ron Kikinis[2]

[1] Computer Science and Artificial Intelligence Lab, MIT, Cambridge, MA, USA.
[2]Surgical Planning Laboratory, Harvard Medical School, Boston, MA, USA.

Abstract. Many neuroanatomy studies rely on brain tissue segmentations of magnetic resonance images (MRI). We present a segmentation tool, which performs this task automatically by analyzing the MRIs as well as tissue specific spatial priors. The priors are aligned to the patient through a non-rigid registration method. The segmentation itself is parameterized by an XML file making the approach easily adjustable to various segmentation problems. The tool is hidden beneath a 'one-button' user interface, which is simple to install and is applicable to a wide variety of image acquisition protocols.

1 Prologue

Our segmentation pipeline (Figure 1) robustly partitions MRIs into grey and white matter, and cortical spinal fluid. The method is guided by tissue specific spatial priors, which define the probability of a tissue class being present at every location within the image. These spatial priors are part of an atlas which is aligned to the MRIs using the non-rigid registration implementation by Guimond [1]. Compared to affine algorithms, non-rigid methods have a reduced risk of systematic biases [2]. The next section will explain in detail the four steps that compose the segmentation pipeline.

2 Segmentation Pipeline

Step 1 - Intensity Normalization: An intensity normalization of the patient MRIs increases the variety of image acquisition protocols that our tool can handle. The simple normalization first determines the average intensity value of the patient MRIs within the head region. We then normalize the MRIs so that the new average intensity value is equivalent to the one defined by the atlas.

Step 2 - Non-Rigid Registration: In order for our atlas to guide the segmentation, it has to be aligned to patient's space. The atlas, a set of MRIs taken on a template subject, is aligned to the patient by registering the template MRIs to the MR scans of the patient, using a non-rigid registration algorithm designed by Guimond et al. [1]. This process results in a correspondence field, which maps each voxel in the atlas space to one in the patient coordinate system (see also Figure 1).

Step 3 - Spatial Prior Alignment: Now that we have determined a correspondence between atlas and patient space we can warp the spatial priors to the patient MRIs. The correspondence field obtained in Step 2 is applied to the spatial priors, resulting in patient specific spatial priors which guide the segmentation of Step 4. In our case, the priors define the spatial distribution of each tissue class over an entire population. The priors were generated by registering labelmaps of 80 different training subjects to a template subject using the method of Warfield et al. [3].

Step 4 - Segmentation: The segmentation of the MRIs is based on EM implementation by [4]. The implementation first reads in the parameters of each tissue class defined by a XML-file. This file can be easily modified to define a different segmentation scenario.

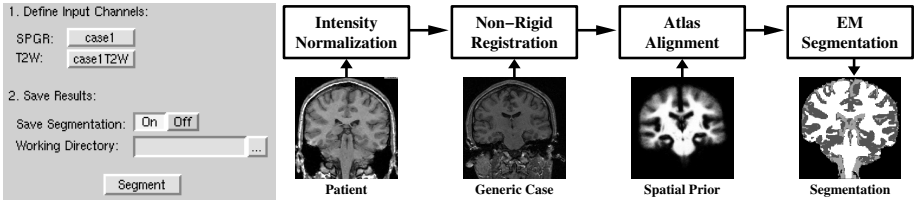

Fig. 1. The simple user interface with the underlying segmentation pipeline for outlining the three major brain tissue classes in MRIs.

After reading in these parameters, the method simultaneously estimates the image inhomogeneities caused by the RF coil and segments the images into the different tissue classes. It improves the solution to both problems by repeating the Expectation Step (E-Step) and Maximization Step (M-Step) until convergence is reached. The E-Step calculates the posterior probability that a voxel is assigned to a tissue class. This calculation is based on the aligned spatial prior, the intensity in the MRIs, and the image inhomogeneity. The M-Step updates the estimate of the image inhomogeneities based on the results of the E-Step. When the algorithm converges, the labelmap at each voxel is defined by the tissue class with the maximum posterior probability at that location.

3 Conclusion

We presented a four step pipeline approach which automatically segments MRIs into the major brain tissue classes. The approach is parameterized by an XML-file that can be adjusted to various segmentation problems. For the neuroscientist, this pipeline is hidden behind a 'one button' user interface (Figure 1). The pipeline is programmed in the Visual Tool Kit (VTK) environment and integrated in the medical imaging software 3D Slicer. 3D Slicer is publicly available (*http:www.slicer.org*) and can be run on several platforms. The segmentation has been tested for both brain tissue classification as well as cortical and subcortical parcellation [4].

Acknowledgments: This investigation was supported by the Department of Veterans Affairs (VA Merit Awards and a REAP Award), and NIH grants K02 MH-01110, R01 MH-50747, P41 RR-13218, and U54-EB-005149.

References

1. A. Guimond, A. Roche, N. Ayache, and J. Meunier, "Three-dimensional multimodal brain warping using the demons algorithm and adaptive intensity corrections," *IEEE Transactions in Medical Imaging*, vol. 20, pp. 58–69, Jan. 2001.
2. S. Srivastava, F. Maes, D. Vandermeulen, W. V. Paesschen, P. Dupont, and P. Suetens, "Effects of anatomical asymmetry in spatial priors on model-based segmentation of the brain MRI: A validation study," in *Medical Image Computing and Computer-Assisted Intervention*, no. 3216 in Lecture Notes in Computer Science, pp. 327–334, Springer-Verlag, 2004.
3. S. Warfield, J. Rexilius, P. Huppi, T. Inder, E. Miller, W. Wells, G. Zientara, F. Jolesz, and R. Kikinis, "A binary entropy measure to assess nonrigid registration algorithm," in *Medical Image Computing and Computer-Assisted Intervention*, pp. 266–274, Oct. 2001.
4. K. Pohl, S. Bouix, R. Kikinis, and W. Grimson, "Anatomical guided segmentation with non-stationary tissue class distributions in an expectation-maximization framework," in *IEEE International Symposium on Biomedical Imaging*, pp. 81–84, 2004.